RESEARCH ARTICLE

Human Mutation

OFFICIAL JOURNAL HGVS HUMAN GENOME VARIATION SOCIETY www.hgvs.org

Pharmacological Chaperoning: A Potential Treatment for PMM2-CDG

Patricia Yuste-Checa,[1] Sandra Brasil,[1] Alejandra Gámez,[1] Jarl Underhaug,[2†] Lourdes R Desviat,[1] Magdalena Ugarte,[1] Celia Pérez-Cerdá,[1] Aurora Martinez,[2*] and Belén Pérez[1*]

[1]Centro de Diagnóstico de Enfermedades Moleculares, Centro de Biología Molecular-SO UAM-CSIC, Universidad Autónoma de Madrid, Campus de Cantoblanco, 28049 Madrid/Centro de Investigación Biomédica en Red de Enfermedades Raras (CIBERER), Instituto de Investigación Sanitaria IdiPAZ, Madrid, Spain; [2]Department of Biomedicine and KG Jebsen Center for Neuropsychiatric Disorders, University of Bergen, Bergen, Norway

Communicated by David Rosenblatt

Received 4 July 2016; accepted revised manuscript 17 October 2016.
Published online 24 October 2016 in Wiley Online Library (www.wiley.com/humanmutation). DOI: 10.1002/humu.23138

ABSTRACT: The congenital disorder of glycosylation (CDG) due to phosphomannomutase 2 deficiency (PMM2-CDG), the most common N-glycosylation disorder, is a multisystem disease for which no effective treatment is available. The recent functional characterization of disease-causing mutations described in patients with PMM2-CDG led to the idea of a therapeutic strategy involving pharmacological chaperones (PC) to rescue PMM2 loss-of-function mutations. The present work describes the high-throughput screening, by differential scanning fluorimetry, of 10,000 low-molecular-weight compounds from a commercial library, to search for possible PCs for the enzyme PMM2. This exercise identified eight compounds that increased the thermal stability of PMM2. Of these, four compounds functioned as potential PCs that significantly increased the stability of several destabilizing and oligomerization mutants and also increased PMM activity in a disease model of cells overexpressing PMM2 mutations. Structural analysis revealed one of these compounds to provide an excellent starting point for chemical optimization since it passed tests based on a number of pharmacochemical quality filters. The present results provide the first proof-of-concept of a possible treatment for PMM2-CDG and describe a promising chemical structure as a starting point for the development of new therapeutic agents for this severe orphan disease.**
Hum Mutat 38:160–168, 2017. © 2016 Wiley Periodicals, Inc.

KEY WORDS: PMM2; CDG; pharmacological chaperones; misfolding proteins

Introduction

Inherited deficiency of phosphomannomutase (congenital disorder of glycosylation [CDG] due to phosphomannomutase 2 deficiency [PMM2-CDG]; MIM# 212065) is a human glycosylation disorder caused by mutations in *PMM2* (MIM# 601785). These lead to reduced phosphomannomutase 2 (PMM2 [E.C.: 5.4.2.8]) activity. PMM2 is a homodimeric enzyme that catalyzes the conversion of mannose-6-phosphate to mannose-1-phosphate, required for lipid-linked oligosaccharide synthesis [Matthijs et al., 2000; Grunewald et al., 2001]. Many mutations affecting *PMM2* give rise to a multisystem clinical spectrum, ranging from mild to severe phenotypes with neonatal death [Grunewald, 2009]. The nervous system is affected in nearly all patients, and commonly involves alternating internal strabismus, psychomotor disability, axial hypotonia, ataxia, strabismus, and hyporeflexia. Other organs may be involved in different ways, leading to failure to thrive, variable dysmorphology, hepatomegaly, skeletal abnormalities, coagulopathy, cardiomyopathy, and hypogonadism [Jaeken, 2010]. Currently, no therapy exists for patients with PMM2-CDG beyond symptomatic treatment. Mortality is as high as 20% in the first years of life [Grunewald, 2009]. Some patients may have up to 40% normal enzymatic activity, whereas heterozygous individuals retain at least 50% catalytic activity and are asymptomatic [Freeze, 2009]. Different therapeutic strategies for PMM2-CDG have been proposed, but have either been unsuccessful or remain far from being tested in patients [Freeze, 2009; Vega et al., 2009; Sharma et al., 2011].

More than 100 disease-causing mutations (mostly missense mutations) have been reported for this gene (HGMD® professional release 2014.3) [Stenson et al., 2014]. We recently described the unstable nature of certain PMM2 folding mutations that retain some residual activity [Yuste-Checa et al., 2015]. These have mostly been reported in a compound heterozygous state (in combination with the most common mutation described for this gene, p.Arg141His, which abolishes catalytic activity). This suggests that PMM2-CDG should be considered a conformational disease [Vega et al., 2009; Yuste-Checa et al., 2015], in which case, pharmacological chaperones (PCs) or proteostasis regulators (PRs) might provide opportunities for therapy. PCs are small molecules that bind to a mutant enzyme and stabilize its native conformation, whereas PRs are small compounds that increase the capacity of the proteostasis network by, for example, increasing the expression of chaperones and thus activating certain protective pathways that increase the folding capacity of the cell [Powers et al., 2009; Muntau et al., 2014]. In recent years, PRs and/or PCs have been shown able to increase enzyme activity by stabilizing defective, misfolded proteins, and reduce

Additional Supporting Information may be found in the online version of this article.

†Present address: Department of Chemistry, University of Bergen, Allégaten 41, Bergen 5007, Norway

*Correspondence to: Belén Perez, Centro de Diagnóstico de Enfermedades Moleculares, Centro de Biología Molecular UAM-CSIC, Universidad Autónoma Madrid, Madrid, Spain. E-mail: bperez@cbm.csic.es; Aurora Martinez, Department of Biomedicine, University of Bergen, Jonas Lies vei 91, 5009-Bergen, Norway. E-mail: Aurora.Martinez@uib.no

Contract Grant Sponsors: Ministerio de Economía y Competitividad (MINECO) (IPT-2012-0561-010000, PI11/01250, PI13/01239); Fundación Gemio; Research Council of Norway (nr. 185181); The KG Jebsen Foundation; NovoSeeds (Novo Nordisk Fonden); Ministerio de Ciencia y Tecnología; European Regional Development Fund.

substrate burden in a number of preclinical models and clinical studies [Gavrin et al., 2012; Muntau et al., 2014]. Indeed, sapropterin dihydrochloride (Kuvan®) has been approved by the Food and Drug Administration and EMEA for the treatment of phenylketonuria [Levy et al., 2007], and tafamidis (Vyndaqel®) approved by the European Medicines Agency (EMEA) for the treatment of transthyretin-related hereditary amyloidosis [Bulawa et al., 2012]. Most PCs are competitive inhibitors of their target enzymes [Desnick and Schuchman, 2002; Fan, 2008], but some have no inhibitory effect at all [Pey et al., 2008; Jorge-Finnigan et al., 2013], allowing for functionality at lower doses [Aymami et al., 2013].

This article reports the use of small molecule library screening to search for novel compounds able to rescue folding-defective PMM2 mutants. Several compounds were identified that stabilized PMM2. The present results pave the way for the treatment of PMM2-CDG via the use of drugs that rescue destabilizing effects.

Materials and Methods

Production of WT-PMM2 and Mutant PMM2 Proteins

The expression plasmid pDEST17-18 encoding human *PMM2* (NM_000303.2, NP000294) plus an N-terminal His_6-tag (Source BioScience, Nottingham, UK) was used to transform *Escherichia coli* strain BL21Star™DE3 One Shot Cells (Invitrogen, Carlsbad, CA). *PMM2* mutations were introduced by site-directed mutagenesis using the QuikChange Mutagenesis Kit (Stratagene, Cedar Drive, TX) and specially designed primers. All products were verified by DNA sequencing. For protein expression, bacteria were grown in modified TYM medium (Studier Auto-Induction Medium [Studier, 2005] with N-Z-amine replaced by tryptone) containing 25 μg/ml zeocine overnight at 37°C. Cells were harvested by centrifugation, resuspended in 20 mM Hepes, 25 mM KCl, 1 mM DTT, pH 7, and 1× Complete Mini, EDTA-free Protease Inhibitor Cocktail (Roche Applied Biosciences, Indianapolis, IN), lysed by sonication, and then centrifuged at 4°C. Protein concentrations were determined following the Bradford method [Bradford, 1976] using the Bio-Rad Protein Assay Reagent (Bio-Rad Laboratories, Munich, Germany). This crude soluble cell extract was used for protein purification.

Protein purification was performed using the ÄKTA Prime System (GE Healthcare, Little Chalfont, UK) at 4°C. The crude extract was loaded onto a HisTrap™ High Performance affinity column (GE Healthcare) equilibrated with 10 mM imidazole, 0.5 M NaCl, 20 mM sodium phosphate, pH 7.4, and eluted with an imidazole gradient from 10 mM to 1 M. The eluted protein fractions were pooled and loaded onto a Superdex 200 HiLoad 16/60 size-exclusion chromatography column (GE Healthcare). The elution fraction corresponding to dimeric PMM2 was recovered and stored for further experiments. The pure protein concentration was estimated by measuring the absorbance at 280 nm in a Nanodrop spectrophotometer (Thermo Scientific, Waltham, MA) using the theoretical molar extinction coefficient estimated from the amino acid composition of HisPMM2 (23,755 M^{-1} cm^{-1}).

High-Throughput Library Screening by Differential Scanning Fluorimetry

Ten thousand compounds of molecular weight 220–547 Da from the MyriaScreen diversity collection, dissolved in DMSO (Sigma–Aldrich, St. Louis, MO) to a final concentration of 2 mg/mL, were screened by DSF, for identification of ligands that stabilize WT-PMM2 thermally [Niesen et al., 2007; Stevens et al., 2010]. This was done by monitoring the thermal denaturation in the presence of the extrinsic fluorescent probe SYPRO Orange (Sigma–Aldrich). Screening was performed by mixing 24 μl purified WT-PMM2 in HEPES-buffer with 1 μl compound in DMSO to a final concentration of 0.064 mg/ml (2.1 μM) WT-PMM2, 20 mM Na-Hepes pH 7.0, 200 mM NaCl, 0.08 mg/ml of compound (average concentration 200 μM), 4% DMSO (compound solvent), and 5× SYPRO Orange, in 384-well RT-PCR plates (Roche Applied Sciences). DMSO controls, with protein but without compounds, were included in each plate. The plates were loaded into a LightCycler480 (Roche Applied Science), and the thermal unfolding curves were recorded from 20°C to 99°C at a scan rate of 2°C/min by following the increase in SYPRO Orange fluorescence intensity associated with protein unfolding ($\lambda_{excitation}$ = 465 nm, $\lambda_{emission}$ = 580 nm). The experimental unfolding curves were then smoothed, normalized, and analyzed using in-house software. The midpoint melting temperature (T_m) was calculated as the temperature at which half of the protein (at relative fluorescence 0.5) was in the unfolded state. The samples were analyzed using in-house software. T_m values from the unfolding curves were recorded in the presence and absence ($T_{m,ref}$) of the compounds and the shift in T_m ($\Delta T_m = T_m - T_{m,ref}$) calculated for each.

In the following validation step, which involved WT-PMM2 and mutant proteins, DSF was also used, but with lower concentrations of the potential PCs (40 and 80 μM). Tests were performed in final reaction volumes of 50 μl, containing 1 μl of the primary hit compound and 2% DMSO in 96-well RT-PCR plates.

For further experiments, larger quantities of the potential PCs selected by the validation steps were purchased from Sigma–Aldrich.

PMM2 Activity Assays

The activity of WT-PMM2 and mutant proteins in the presence of the selected potential PCs was assayed using the method of Van Schaftingen and Jaeken (1995), as modified by de Koning et al. (1998).

For the calculation of IC_{50} values, pure WT-PMM2 was used. Fifty nanograms of nanodrop-measured pure dimeric PMM2 (molar extinction coefficient 23,755 M^{-1} cm^{-1}) were incubated with 1 μl of one of four selected potential PCs (compounds IV, VI, VI, and VIII) at different concentrations, along with 0.5% BSA, for 10 min at 30°C. The following activity assay was performed as above. The corresponding DMSO controls were included in the assay. The IC_{50} values for the inhibitory compounds were calculated using nonlinear regression (GraphPad Prism 6 software) by plotting the log concentration of the compounds (*M*) versus WT-PMM2 enzyme activity (%).

PMM2 activity assays involving patient-derived fibroblasts overexpressing different folding mutations were performed as described elsewhere [Yuste-Checa et al., 2015].

Evaluation of the Effects of four Selected Potential PCs on PMM2 Stability by Degradation time Course

Dimeric PMM2 used for thermal stability analysis was produced by the RTS 100 *E. coli* HY Kit transcription-translation-coupled system (5 PRIME, Hilden, Germany), following the manufacturer's recommendations. To produce PMM2 proteins, the reaction mix provided by the kit, together with 500 ng of the corresponding expression vector and 1 μl of each selected potential PC at different concentrations, were incubated for 30 min at 30°C. The reaction was then stopped by adding 1 μl of DNase (1 mg/ml) and 1 μl of RNase (1 mg/mL). It was then further incubated at 37°C, and

1.5 μl aliquots removed at different times. Samples were subjected to electrophoresis in 10% NuPAGE® Bis-Tris Precast Gels (Invitrogen). ProSieve® Color Protein Markers (Lonza, Basel, Switzerland) were used as molecular weight markers. Proteins were transferred to a nitrocellulose membrane using the iBlot® Dry Blotting System (Invitrogen). Membranes were blocked for at least 1 hr with 0.05% PBS-Tween and 5% low fat milk. Immunodetection was performed using primary mouse polyclonal antibodies to PMM2 protein (Abnova; H00005373-A01) and polyhistidine (Sigma–Aldrich; H1029). Conjugated goat-anti mouse immunoglobulin G (IgG)-horseradish peroxidase (Santa Cruz Biotechnology, Santa Cruz, CA) was used as the secondary antibody. The Enhanced Chemiluminescence System (GE Healthcare) was used as the detection method. Relative amounts of protein were determined by densitometry using a Bio-Rad GS710 Calibrated Imaging Densitometer running Quantity One 4.3.1 software (Bio-Rad Laboratories).

Cellular Model used to Examine PMM2 Activity in the Presence of four Selected Potential PCs

Patient-derived fibroblasts P1 (p.Arg141His/p.Asp65Tyr), P2 (p.Pro113Leu/p.Pro113Leu), P3 (p.Arg141His/p.Arg162Trp) and P4 (c.640-9T>G/p.Thr237Met) were grown from skin biopsies (taken with informed consent) following standard conditions in minimal essential medium supplemented with 1% glutamine, 10% fetal calf serum, and antibiotics. These cells were then immortalized using pBABE-puro containing SV40 DNA sequences. GM08680 healthy-derived fibroblasts (Coriell Institute for Medical Research, NIGMS Human Genetic Cell Repository, Camden, NJ) were used as a control.

All four patient-derived fibroblast lines were transduced with their own folding or oligomerization mutation, that is, p.Asp65Tyr, p.Pro113Leu, p.Arg162Trp, and p.Thr237Met for P1, P2, P3, and P4, respectively. Control-derived fibroblasts were transduced with WT-PMM2. The full-length ORF of human *PMM2* was cloned into the mammalian lentiviral plasmid pReceiver-Lv101 (EX-M0134-Lv101) (GeneCopoeia, Rockville, MD), which contains the FLAG tag preceding the multiple cloning site. Lentiviral stock production and fibroblast infection were performed as described elsewhere [Yuste-Checa et al., 2015]. Efficiently infected fibroblasts were selected by Geneticin treatment.

Structural Analysis of the Hit Compounds

The physicochemical and absorption, distribution, metabolism, and excretion (ADME) properties of the hits were evaluated using QikProp, v.2.1 software (Schrödinger, LLC, New York, NY) and ChemBioDraw Ultra 14 Suite software (PerkinElmer, Inc. Waltham, MA). The pharmacochemical analysis of the compounds was performed using the SmartsFilter program (http://pasilla.health.unm.edu/tomcat/biocomp/smartsfilter). All analyses were performed under the "normal" and "analyze one molecule" modes. The SMARTS (http://www.daylight.com/dayhtml/doc/theory/theory.smarts.html) sets used were: Glaxo, Blake, ALARM NMR, PAINS, and Oprea [Hann et al., 1999; Oprea et al., 2002; Blake, 2005; Huth et al., 2005, Baell and Holloway, 2010].

Structural Model of PMM2

The structural model of the human PMM2 protein, as well as the location of the residues affected by the selected missense mutations, was prepared using the PyMOL Molecular Graphics System v.1.7.4 program (Schrödinger LLC) and the crystal coordinates of PMM2 (PDB ID 2AMY).

Statistics

Statistical analyses were performed using IBM SPSS Statistics v.21 software for Windows. One-way ANOVA followed by a Bonferroni *post hoc* test or the two-tailed Student's *t*-test were used to compare the PMM2 activities and stabilities measured by DSF and the degradation time course assays. Data are reported as the mean ± SD.

The research was reviewed and approved by a duly constituted ethics committee.

Results

High-Throughput Screening of Possible PCs

Ten thousand small-molecular-weight compounds from a commercial library were screened by differential scanning fluorimetry (DSF) at 80 μg/ml (average concentration of the compounds 200 μM) to search for molecules with PC potential, that is, capable of increasing the thermal stability of human wild-type PMM2 (WT-PMM2). Stabilization was evaluated by comparing the melting temperatures (T_m) of pure WT-PMM2 (51.6 ± 0.1°C) in the absence and presence of the possible PCs and calculating the shift in the T_m (thermal shift; ΔT_m). Eight compounds stabilized PMM2 by ≥1°C, indicating binding of the compounds [Niesen et al., 2007]. The analysis revealed eight hit compounds (compounds I–VIII). Most were associated with a ΔT_m of between 1°C and 3°C, whereas compound IV was associated with a ΔT_m of 16°C (Figs. 1 and 2 and Table 1).

The stabilizing effect on pure WT-PMM2 of the eight compound hits was then tested at 40 and 80 μM, that is, at concentrations that might be used in cell systems. A stabilizing effect of compounds I, II, III, and V ($\Delta T_m \geq 1$°C) was observed only at the highest concentration (200 μM). Compounds IV, VI, VII, and VIII increased PMM2 stability at 40 μM and compounds IV, VII, and VIII did so also at 80 μM, although the saturation point may already have been passed (Table 1).

Effect of the Potential PCs on the Activity of WT-PMM2

Given their concentration-dependent thermal stabilization of WT-PMM2, compounds IV, VI, VII, and VIII appeared promising as potential PCs and were selected for further studies with PMM2 mutants. The optimal concentration was determined for each; IC_{50} values of approximately 130 μM were obtained for compounds IV and VI, and 280 μM for compound VII (Fig. 3). The IC_{50} values obtained confirmed the 40 and 80 μM concentrations of compounds to have very little inhibitory effect under the assay conditions used. Compound VIII seemed not to have any inhibitory effect on PMM2 activity at any of the tested concentrations (the highest being 2.5 mM) (Fig. 3).

Effect of the Four Selected Potential PCs on the Stability of Mutant PMM2

To determine whether the four selected potential PCs could act as such for unstable PMM2 mutants, their effect on the stability of different PMM2 mutants was studied by DSF. The selected mutants,

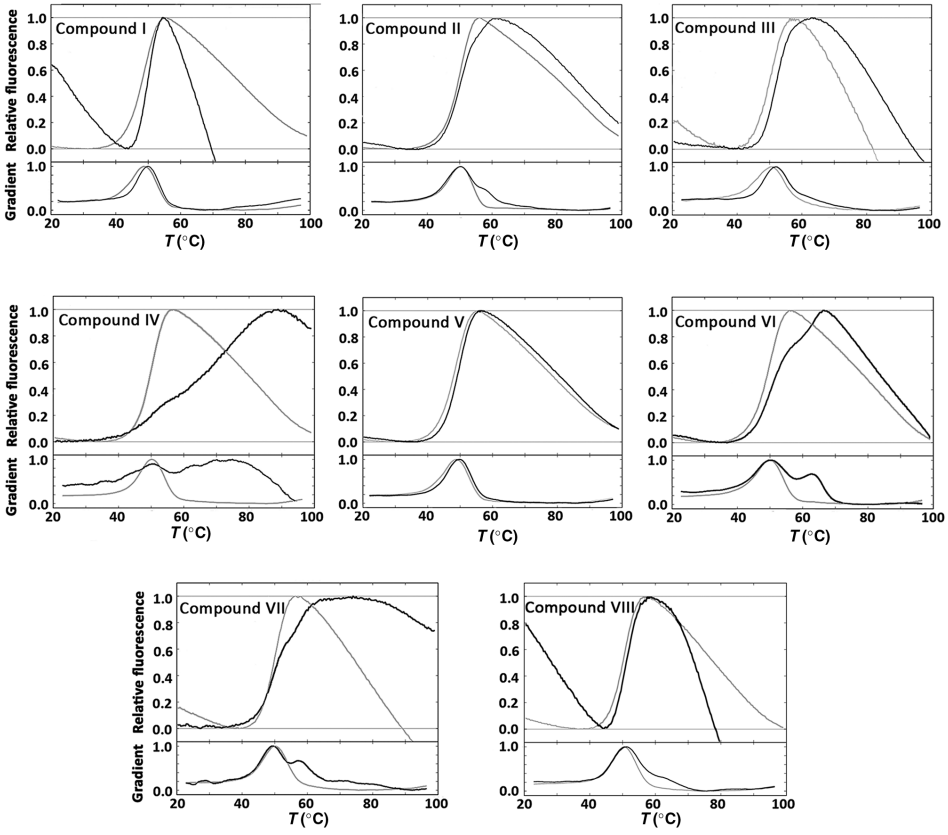

Figure 1. Differential scanning fluorimetry profiles for the eight compound hits that stabilize PMM2, identified by high-throughput screening. Thermal denaturation profiles of pure dimeric WT-PMM2 (fluorescence at 610 nm vs. temperature T [°C]), in the absence (gray) or presence of compounds I–VIII at 0.08 mg/mL (black), all with 4% DMSO.

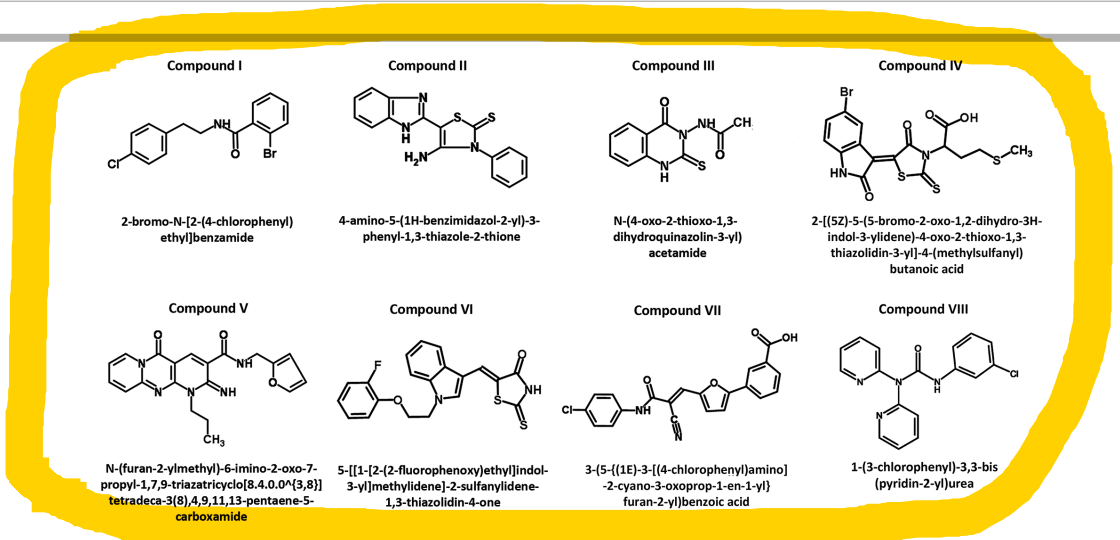

Figure 2. Chemical structures and IUPAC names of the eight hit compounds obtained by high-throughput screening (compounds I–VIII).

p.Val44Ala, p.Asp65Tyr, p.Arg123Gln, p.Arg141His, p.Arg162Trp, p.Thr237Met, and p.Cys241Ser (see location in the PMM2 structure in Supp. Fig. S1), which cause misfolding, are prevalent in the Spanish population [Perez et al., 2011; Yuste-Checa et al., 2015]. Recombinant enzyme was used in these assays and the limitation to the compound concentrations was their solubility.

All four compounds had a significant stabilizing effect on all the tested mutants, with a T_m shift of their PMM2 between 1.5°C and 45.1°C (Supp. Fig. S2 and Table 2). Some data could not be collected because of the poor curves obtained (the result of quenching of the fluorescence in some cases, especially for compound VII). The greatest stabilization effect was observed for compound IV, which increased the T_m of the mutant proteins by 25.7°C–45.1°C (Table 2), surpassing the basal WT-PMM2 T_m (Supp. Fig. S2). Compound VII was also able to increase the T_m of all the mutants by 2.1°C–31.7°C (Table 2), in most cases also beyond the WT-PMM2 T_m baseline

Table 1. Thermal Stabilization of WT-PMM2 by the Initial Eight Hit Compounds (Compounds I–VIII) Determined by DSF

Compound	DSF (ΔT_m, °C)		
	Initial HT[a] screening (average for all compounds, 200 μM)	Validation at 80 μM	Validation at 40 μM
I	1.8 (236 μM)	0.07 ± 0.07	**0.13 ± 0.05****
II	1 (247 μM)	–0.6 ± 0.06	–0.7 ± 0.04
III	2.2 (340 μM)	–0.2 ± 0.04	–0.25 ± 0.05
IV	16.1 (169 μM)	**29.1 ± 0.6*****	**25.4 ± 0.6*****
V	1.1 (212 μM)	–0.2 ± 0.07	–0.2 ± 0.1
VI	2.7 (201 μM)	**0.45 ± 0.15*****	0 ± 0.2
VII	1.1 (204 μM)	**3.35 ± 0.35*****	**2.7 ± 0.1*****
VIII	1.1 (246 μM)	**2 ± 0.3*****	**1.5 ± 0.1*****

ΔT_m (°C) was calculated as the difference between the T_m recorded in the presence of the compound and that recorded for the DMSO controls.
[a]HT, high-throughput.
DMSO present in all samples at 4% in the initial HT screening, and at 2% in the validations (DSF).
*** $P < 0.001$ (differences with respect to DMSO controls).
** $P < 0.01$ (differences with respect to DMSO controls).
Significant differences in T_m compared with DMSO controls are shown in bold.

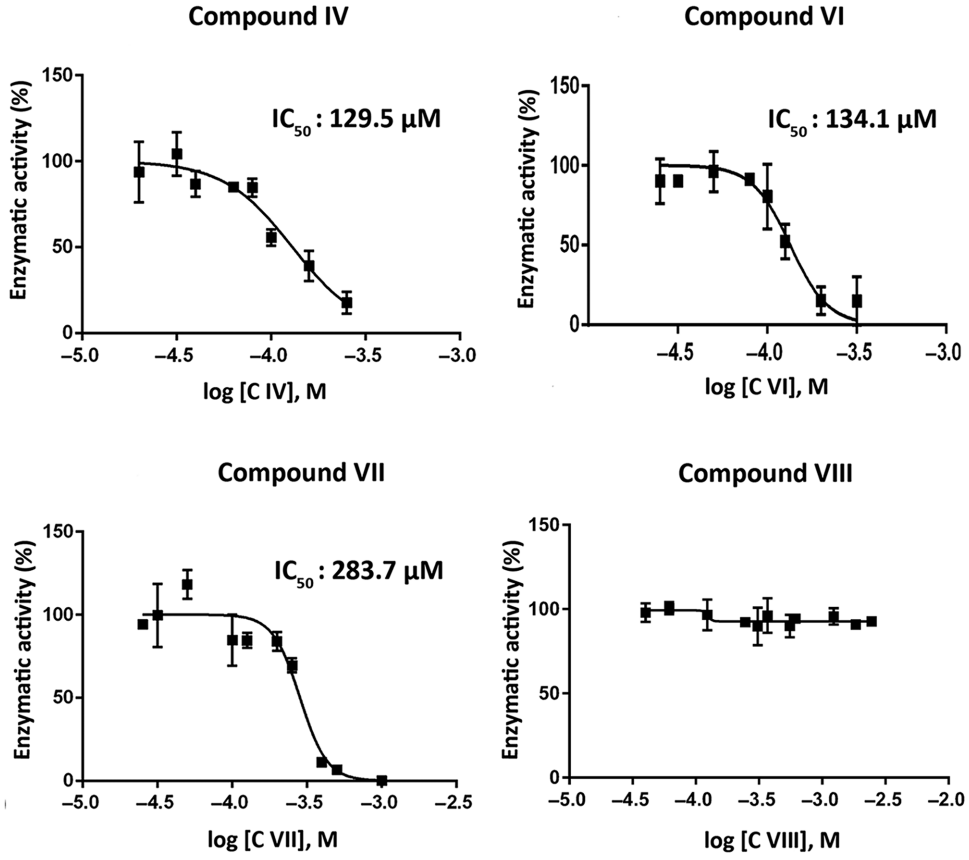

Figure 3. Dose–response curves for pure, dimeric WT-PMM2 and the four selected potential PCs (compounds IV, VI, VII, and VIII). The data represent PMM2 enzyme activity (as a percentage of the DMSO control result) versus the log concentration of the compounds (*M*). IC_{50} values for each compound are also indicated, except for compound VIII given its apparent lack of any inhibitory effect on the activity of the pure WT PMM2 protein.

(Supp. Fig. S2). A smaller but also statistically significant T_m shift was obtained for compound VI (1.5°C–4.5°C) and compound VIII (2.1°C–6.5°C) (Table 2). For the p.Arg123Gln and p.Thr237Met mutants incubated with compound VI, the T_m shift achieved was the same as that seen for WT-PMM2. The same was also seen for p.Asp65Tyr, p.Arg123Gln, p.Arg162Trp, and p.Thr237Met when incubated with compound VIII (Supp. Fig. S2).

The four selected potential PCs were further subjected to assessment of their stabilizing ability (at 40 and 80 μM) by determining the half-life of both WT-PMM2 and mutant PMM2 in a prokaryotic transcription–translation-coupled system. Whereas DSF is the method of choice for high-throughput (HT) selection and validation of hits, and values are measured using purified recombinant enzyme, the protein half-life assay is performed with cellular

extracts (in vitro transcription–translation system) and contributes evidence regarding the protection from aggregation and proteasomal degradation. These are properties that a priori may represent a phenomenological effect of intracellular stabilization beyond that of increased thermal stability.

The selected mutants were three representative folding mutants, p.Asp65Tyr, p.Arg162Trp, p.Thr237Met, also included in the DSF assays (Supp. Fig. S2) and the oligomerization mutant p.Pro113Leu (Supp. Fig. S1) [Yuste-Checa et al., 2015]. All four potential PCs increased the stability of WT-PMM2 and all mutants, increasing their half-lives 1.4–6 times (with the exception of WT-PMM2 and the p.Arg162Trp mutant when incubated with compound VII) (Table 3). The increase in the half-life of the mutant proteins, at least at one of the tested concentrations, afforded them a longer half-life than recorded for WT-PMM2 (Supp. Fig. S2).

Together, the DSF and degradation time course results thus suggest that compounds IV, VI, VII, and VIII have a broad effect on the tested unstable mutants, that is, not a PMM2-mutant-specific stabilizing effect.

Effect of the four Selected Potential PCs on the Activity of Different PMM2 Mutants in a Cellular Model of PMM2-CDG

PMM2 activity assays were performed with soluble cell extracts from healthy control and patient-derived fibroblasts overexpressing WT-PMM2 or PMM2 made unstable by the mutations p.Asp65Tyr, p.Pro113Leu, Arg162Trp, and p.Thr237Met (Supp. Fig. S1) [Yuste-Checa et al., 2015]. The cells were incubated for 48 hr with different concentrations of compounds IV, VI, VII, and VIII. The concentrations used were selected based on the effect of the compounds on the growth of healthy control fibroblasts (data not shown). Thus, concentrations of >20 μM were avoided.

An increase in enzyme activity was achieved by all four compounds in patient-derived cells overexpressing any of the mutant proteins, at least at one of the tested concentrations (Supp. Fig. S3). For compounds IV, VI, VII, and VIII, the increases ranged from 1.3 to 1.4, 1.2 to 2.1, 1.3 to 1.7, and 1.2 to 1.7 times the baseline activity recorded for each cell line, respectively (Supp. Fig. S3).

The greatest activity increase in the cell line overexpressing the p.Asp65Tyr mutant was observed with compound VI at 20 μM (from a baseline [compared with WT-PMM2] of 28% to 58%). In the case of the p.Pro113Leu-overexpressing cells, compound VII at 20 μM and compound VIII at 10 μM produced an increment from a baseline of 19% to about 30%. In the p.Arg162Trp-overexpressing cells, compounds VI and VII at 20 μM, and compound VIII at 10 μM, increased the activity from a baseline of 13% to 19%. Finally, compound VIII, at 10 μM, showed the greatest activity of all in the cell line overexpressing the p.Thr237Met mutant—from a baseline of 53% to 84% (Table 4). It should be noted that compound VI at 20 μM significantly increased the control cell line activity by 1.2 times (Supp. Fig. S3).

Western blotting of overexpressed PMM2 was performed with soluble cell extracts from the different cell lines incubated with compound VII at 20 μM, and compound VIII at 2 and 10 μM, but no significant increases in protein were observed (data not shown).

Structural Analysis of the Hit Compounds

Analysis of the structures of the selected hits (Fig. 2) revealed good physicochemical and ADME properties for compounds IV, VI, VII, and VIII (Supp. Table S1). These structures were also chemically analyzed by the SmartsFilter program (available online), which uses Smiles Arbitrary Target Specification (SMARTS) queries, the same system used by pharmaceutical companies to specify substructures of interest. Of the four selected hits, only compound VIII passed all filters; compounds IV, VI, and VII failed two or more filters (Supp. Table S2). As rhodanine derivatives, compounds IV and VI belong to the pan assay interference compounds (PAINS) [Baell and Holloway, 2010], which often show a broad and non-specific spectrum of biological activity [Tomasic and Peterlin Masic, 2012]. Compound VII failed the ALARM NMR filter, suggesting it to be thiol-reactive [Huth et al., 2005].

Discussion

PMM2-CDG is the most common CDG, occurring at an estimated frequency of about 1/20,000 [Freeze et al., 2014]. Currently, there is no efficient treatment for this severe disorder. Many therapeutic approaches have been proposed, such as gene therapy or enzyme- or product-replacement therapy [Freeze, 2009], but all of them present serious problems.

It is of note that 80% of all reported PMM2 mutations are missense mutations (HGMD® professional release 2014.3, http://www.hgmd.cf.ac.uk/ac/index.php) [Stenson et al., 2014]. A recent, comprehensive functional mutation analysis has suggested that the loss of function of most of the studied missense mutant proteins revolves around an increased susceptibility to degradation and/or aggregation, a common mechanism operating in conformational diseases [Vega et al., 2009; Yuste-Checa et al., 2015]. The present study describes how PCs can stabilize normal and mutant PMM2 proteins, and in some cases increase mutant PMM2 activity, in a cellular disease model. The results satisfy the first stage in the development of a new strategy for treating PMM2-CDG. Indeed, PCs might be used to treat a broad range of patients with PMM2-CDG since most are compound heterozygous with one severe null mutation and one destabilizing mutation retaining some residual activity [Perez et al., 2011; Yuste-Checa et al., 2015].

Initial HT screening for selecting compounds based on increased thermal stability for recombinant proteins is an effective means of discovering stabilizing molecules [Pey et al., 2003; Jorge-Finnigan et al., 2013]. At the starting point of the present pipeline, two complementary approaches were used. Whereas DSF is the method of choice for HT selection and validation of hits, and values are measured using purified recombinant enzyme, the protein half-life is performed with multiproteic extracts and contributes evidence regarding the protection from aggregation and proteasomal degradation. These are properties that a priori may represent a phenomenological effect of intracellular stabilization beyond that of increased thermal stability. Despite the differences in the effects of compounds as measured by these two methods, notably with respect to their concentration-dependent effect, it is reassuring that the selected hits based on the thermal stability of PMM2, that is, IV, VI, VII, and VIII (Table 1), also stabilized the protein in the half-life essay. When positive effects on the stability of the mutants were observed in the thermal melting assays, they were also seen in the enzyme assays in cells. However, the large effect of compound IV on the thermal stability of the mutants does not correlate with the activity results obtained in fibroblast. This is probably due to the intrinsic differences between the two methods. In any event, it is only upon validation, via functional assays and the use of pharmacochemical quality filters, that any compound can be further selected as a promising PC. Thus, at the end of the pipeline, compounds VII

Table 2. Effect of the Selected Potential PCs (Compounds IV, VI, VII, and VIII) on the Thermal Stability of WT-PMM2 and PMM2 Mutants (p.Val44Ala; p.Asp65Tyr, p.Arg123Gln, p.Arg141His, p.Arg162Trp, p.Thr237Met, and p.Cys241Ser), as Determined by DSF

		DSF (ΔT_m, °C)							
		WT	p.Val44Ala	p.Asp65Tyr	p.Arg123Gln	p.Arg141His	p.Arg162Trp	p.Thr237Met	p.Cys241Ser
Compound IV	**40 μM**	25.4 ± 0.6***	35.9 ± 0.9***	37.2 ± 0.8***	25.7 ± 1.5***	35.3 ± 0.5***	35.3 ± 1.2***	34.8 ± 0.9***	33.2 ± 0.6***
	80 μM	29.1 ± 0.6***	44.1 ± 0.4***	45.1 ± 0.5***	36 ± 0.5***	42.5 ± 0.2***	41.6 ± 0.4***	42 ± 0.5***	41.2 ± 0.3***
Compound VI	**40 μM**	–0.9 ± 0.2	4.1 ± 0.5***	3.4 ± 0.5***	1.5 ± 0.1***	1.8 ± 0.3***	1.6 ± 0.5***	2.4 ± 0.1***	n.d.
	80 μM	0.45 ± 0.15***	4.5 ± 0.4***	4.3 ± 0.9***	2.1 ± 0.4***	3.5 ± 1.2**	1.7 ± 0.4***	3.8 ± 0.8***	4 ± 2.4***
Compound VII	**40 μM**	2.7 ± 0.1***	14.6 ± 2.7***	14.4 ± 3.6***	2.1 ± 0.4***	4.2 ± 2.7*	9.5 ± 2.14***	9 ± 1.5***	n.d.
	80 μM	3.35 ± 0.35***	26.3 ± 1.6***	31.7 ± 12.5***	n.d.	n.d.	22.8 ± 3.3***	n.d.	n.d.
Compound VIII	**40 μM**	1.5 ± 0.1***	3.1 ± 0.6***	4.1 ± 0.4***	2.1 ± 0.1***	3.4 ± 0.2***	2.4 ± 0.1***	2.7 ± 0.4***	3.2 ± 0.2***
	80 μM	2 ± 0.3***	5.3 ± 0.5***	6.5 ± 0.6***	2.8 ± 0.1***	3.7 ± 0.4***	3.3 ± 0.2***	4.1 ± 0.2***	3.9 ± 0.2***

ΔT_m (°C) was calculated as the difference between the T_m recorded in the presence of the compound and that recorded for the DMSO controls.
Data represent the mean + SD of at least three independent experiments.
n.d., not determined.
*** $P < 0.001$(differences with respect to DMSO controls).
** $P < 0.01$ (differences with respect to DMSO controls).
* $P < 0.05$ (differences with respect to DMSO controls).

Table 3. Effect of the Selected Potential PCs (Compounds IV, VI, VII, and VIII) on the Thermal Stability of WT-PMM2 and PMM2 Mutants (p.Asp65Tyr, p.Pro113Leu, p.Arg162Trp, p.Thr237Met) as Determined by Degradation Time Courses Analysis

		Degradation time course				
		WT	p.Asp65Tyr	p.Pro113Leu	p.Arg162Trp	p.Thr237Met
Compound IV	**40 μM**	**2.22 ± 0.52****	**3.75 ± 0.15*****	**5.24 ± 1.09****	**2.86 ± 1.09***	**1.69 ± 0.31**
	80 μM	**1.60 ± 0.25****	**5.37 ± 0.5*****	**2.77 ± 0.86***	**3.10 ± 0.41*****	**3.04 ± 0.29****
Compound VI	**40 μM**	**1.37 ± 0.06****	**3.27 ± 0.27*****	**2.02 ± 0.11*****	**3.81 ± 1*****	**4.61 ± 0.51*****
	80 μM	0.93 ± 0.27	**4.9 ± 0.76*****	**3.86 ± 0.79*****	**6.05 ± 0.45*****	**3.3 ± 0.56****
Compound VII	**40 μM**	1.31 ± 0.19	**5.23 ± 1.61***	**2.87 ± 0.61***	1.32 ± 0.23	**2.49 ± 0.39***
	80 μM	0.94 ± 0.15	**4.29 ± 0.61*****	**2.07 ± 0.14****	1.35 ± 0.36	**3.49 ± 0.09*****
Compound VIII	**40 μM**	**1.69 ± 0.26****	**4.63 ± 0.45*****	2.10 ± 0.72	**3.04 ± 0.84***	**2.28 ± 0.53***
	80 μM	**1.98 ± 0.74***	**3.52 ± 0.73****	**2.96 ± 0.65***	**2.79 ± 0.68****	**3.09 ± 0.59****

Relative half-lives of each protein incubated with the compounds compared with the protein half-life of DMSO controls.
Data represent the mean + SD of at least three independent experiments.
*** $P < 0.001$ (differences compared with DMSO control).
** $P < 0.01$ (differences compared with DMSO control).
* $P < 0.5$ (differences compared with DMSO control).

Table 4. Activity Values for the WT-PMM2 and Mutant PMM2 Cell Lines (Healthy and Patient-Derived Fibroblast Overexpressing WT Protein and the p.Asp65Tyr, p.Pro113Leu, p.Arg162Trp, and p.Thr237Met Folding Mutations, respectively) Incubated with the Optimal Concentration of each Selected Potential PC (Compounds IV, VI, VII, and VIII): Comparisons with Baseline Activity of the WT-PMM2 Cell Line (Taken as 100%)

		Control (WT)	P1 (p.Asp65Tyr)	P2 (p.Pro113Leu)	P3 (p.Arg162Trp)	P4 (p.Thr237Met)
		100 ± 1.72	27.9 ± 1.8	19 ± 8	13.3 ± 2.8	53.4 ± 8.6
Compound IV	**0.1 μM**	107.7 ± 9.1	38.6 ± 8.1*	24.9 ± 1.3***	17.4 ± 2.8**	67.4 ± 6.8**
Compound VI	**20 μM**	118.3 ± 17.8*	58 ± 17.4**	21.3 ± 6.3	18.5 ± 3.9*	79.2 ± 16.9**
Compound VII	**20 μM**	101 ± 14.4	41.1 ± 12.1**	29.8 ± 6.5**	18.6 ± 2.2**	75 ± 16.4**
Compound VIII	**2 μM**	88 ± 15.5	36.8 ± 5***	32.5 ± 12.2*	16.2 ± 0.8*	69.9 ± 8**
	10 μM	103.6 ± 2.1	27.9 ± 4.2	28.9 ± 4.9***	19.1 ± 3**	83.8 ± 12.3**

Data represent the mean + SD of at least three independent experiments.
*** $P < 0.001$ (differences in the activity of the compounds compared with the corresponding baseline).
** $P < 0.01$ (differences in the activity of the compounds compared with the corresponding baseline).
* $P < 0.05$ (differences in the activity of the compounds compared with the corresponding baseline).

and notably VIII, but not compound IV, were selected for further derivatization.

In the cellular model of the disease, compounds IV, VI, VII, and VIII significantly increased the activity of the p.Asp65Tyr, p.Pro113Leu, p.Arg162Trp, and p.Thr237Met PMM2 mutants (allele prevalence about 30% in the Spanish and Portuguese populations) [Perez et al., 2011] by between 1.2 and 2.1 times the baseline value, increasing them to 58%, 30%, 19%, and 84%, respectively. It is encouraging that in the activity assays with the fibroblasts, even at 0.4 μM—much lower than the toxicity limit—compound VIII had a positive effect on enzyme activity in cultured cells. Notably, compound VIII increased the enzymatic activity of p.Pro113Leu, p.Arg162Trp, and p.Thr237Met by 1.5 times at this concentration. Hit-to-lead derivatization of compound VIII will be focused on reducing its toxicity and possible off-target effects.

It would appear that compounds IV, VI, VII, and VIII have a broad range effect rather than mutant-specific effect. All four compounds showed a positive effect on the stability and activity of the p.Pro113Leu mutant (a type of mutation causing dimer disruption that is particularly difficult to treat), increasing its half-life between 2.0 and 5.2 times, and its activity between 1.3 and 1.6 times its baseline value. Such results broaden the mutational spectrum for

which these potential PCs could be used—including oligomerization mutants among others. It should be taken into consideration that the second most common PMM2 mutation is the oligomerization mutant-causing p.Phe119Leu [Schollen et al., 2000; Andreotti et al., 2013].

Over the last few years, academic researchers have become aware of the critical limitations of certain classes of compounds in commercial chemical libraries as starting points for optimization [Dahlin et al., 2015]; [Dahlin and Walters, 2014]; [Baell and Walters, 2014]. Their abundance in such commercial libraries, plus the fact that they usually show apparent great activity toward many targets, can make them look more promising than they may actually be [Baell and Walters, 2014]. The present analysis of the four selected chemical structures using different computational filters raised warnings regarding compounds IV and VI, which fell into the PAINS category; they should, therefore, not be considered priority compounds in drug discovery studies [Baell and Holloway, 2010; Baell and Walters, 2014]. However, in some cases, ligand promiscuity has also been associated with successful optimization outcomes [Che et al., 2012]. While compound VII did not fall into the PAINS category, it was flagged as ALARM NMR positive, indicating it to have a thiol-reactive structure—and as such to be a potential pharmaceutical dead end [Huth et al., 2005]. Compound VIII was negative for all the computational filters tested, showing it to possess a chemical structure that might be optimized in order to improve its ADME/PK (pharmacokinetics) profile, and its activity, and apparently amenability to chemical derivatization for eliminating any cytotoxicity, thus rendering it able to rescue the activity of PMM2 in patients. Indeed, the results of the computational triage performed for compound VIII, together with its apparent lack of any inhibitory effect on the enzymatic activity of pure WT protein, plus its positive effect on the stabilization and activity of the PMM2 mutants, render it the most promising for optimization and eventual clinical use. Future work should include this optimization and testing in animal models.

We have recently reported that the missense mutations p.Phe118Leu and p.Arg137His, present in the PMM2-CDG mouse model described by other authors [Schneider et al., 2012], are not pure destabilizing mutations [Yuste-Checa et al., 2015]. Thus, no completely appropriate PMM2-CDG animal model is available for testing putative PCs. However, as described for other diseases, the production of induced pluripotent stem cells from patients that can be programmed to produce specific cell types offers a promising alternative for testing potential PCs [Tiscornia et al., 2013; Panicker et al., 2014].

Given the multisystem phenotype associated with PMM2-CDG, potential PCs would need to be systemically distributed; certainly, they would need to reach the central nervous system, especially the cerebellum [Grunewald, 2009]. Compound VIII, shows a lipophilicity value (clogP) that predicts good permeability in this respect [Summerfield et al., 2007]. Crossing the blood–brain barrier increases the likelihood of improving the neurological symptoms of PMM2-CDG, such as cerebellar atrophy [Serrano et al., 2015]. However, it should be taken in consideration that glycoproteins are involved in multiple signaling pathways essential in tissue and organ development [Thiel et al., 2006; Grunewald, 2009; Schneider et al., 2012]. The success of any treatment would therefore depend on early diagnosis.

Recently, the coadministration of PCs and PRs has been described to exert a synergistic effect in the restoration of mutant enzyme function in fibroblasts derived from patients with different lysosomal storage diseases [Mu et al., 2008]. This opens up the possibility of combining two mechanistically distinct solutions.

In summary, this work reports the first proof-of-concept of the use of PCs in the treatment of PMM2-CDG, and provides the basis for developing a new therapy based on the chemical structure of compound VIII. Its chemical optimization could be addressed to improve its therapeutic potential, perhaps allowing this severe orphan disease to be treated for the first time.

Abbreviations

CDG, congenital disorder of glycosilation; PMM2, phosphomannomutase 2; PCs, pharmacological chaperones; DSF, differential scanning fluorimetry; PRs, proteostasis regulators; HGMD, Human Gene Mutation Database; EMEA, European Medicines Agency; T_m, melting temperature; SMARTS, Smiles Arbitrary Target Specification; PAINS, pan assay interference compounds; ADME/PK, absorption, distribution, metabolism, and excretion and pharmacokinetics; HT, high-throughput

Acknowledgments

We wholeheartedly thank the Spanish families affected by PMM2-CDG who actively participated in this work (aesCDG). We also thank Minoryx Therapeutics S.L. for advice on the structural analysis of the hits.

Disclosure statement: The authors declare no conflict of interest.

References

Andreotti G, Pedone E, Giordano A, Cubellis MV. 2013. Biochemical phenotype of a common disease-causing mutation and a possible therapeutic approach for the phosphomannomutase 2-associated disorder of glycosylation. Mol Genet Genomic Med 1:32–44.

Aymami J, Barril X, Rodriguez-Pascau L, Martinell M. 2013. Pharmacological chaperones for enzyme enhancement therapy in genetic diseases. Pharm Pat Anal 2:109–124.

Baell J, Walters MA. 2014. Chemistry: Chemical con artists foil drug discovery. Nature 513:481–483.

Baell JB, Holloway GA. 2010. New substructure filters for removal of pan assay interference compounds (PAINS) from screening libraries and for their exclusion in bioassays. J Med Chem 53:2719–2740.

Blake JF. 2005. Identification and evaluation of molecular properties related to preclinical optimization and clinical fate. Med Chem 1:649–655.

Bradford MM. 1976. A rapid and sensitive method for the quantitation of microgram quantities of protein utilizing the principle of protein-dye binding. Anal Biochem 72:248–254.

Bulawa CE, Connelly S, Devit M, Wang L, Weigel C, Fleming JA, Packman J, Powers ET, Wiseman RL, Foss TR, Wilson IA, Kelly JW, Labaudinière R. 2012. Tafamidis, a potent and selective transthyretin kinetic stabilizer that inhibits the amyloid cascade. Proc Natl Acad Sci USA 109:9629–9634.</bib>

Che J, King FJ, Zhou B, Zhou Y. 2012. Chemical and biological properties of frequent screening hits. J Chem Inf Model 52:913–926.

Dahlin JL, Nissink JW, Strasser JM, Francis S, Higgins L, Zhou H, Zhang Z, Walters MA. 2015. PAINS in the assay: chemical mechanisms of assay interference and promiscuous enzymatic inhibition observed during a sulfhydryl-scavenging HTS. J Med Chem 58:2091–2113.

Dahlin JL, Walters MA. 2014. The essential roles of chemistry in high-throughput screening triage. Future Med Chem 6:1265–1290.

de Koning TJ, Dorland L, van Diggelen OP, Boonman AM, de Jong GJ, van Noort WL, De Schryver J, Duran M, van den Berg IE, Gerwig GJ et al. 1998. A novel disorder of N-glycosylation due to phosphomannose isomerase deficiency. Biochem Biophys Res Commun 245:38–42.

Desnick RJ, Schuchman EH. 2002. Enzyme replacement and enhancement therapies: lessons from lysosomal disorders. Nat Rev Genet 3:954–966.

Fan JQ. 2008. A counterintuitive approach to treat enzyme deficiencies: use of enzyme inhibitors for restoring mutant enzyme activity. Biol Chem 389:1–11.

Freeze HH. 2009. Towards a therapy for phosphomannomutase 2 deficiency, the defect in CDG-Ia patients. Biochim Biophys Acta 1792:835–840.

Freeze HH, Chong JX, Bamshad MJ, Ng BG. 2014. Solving glycosylation disorders: fundamental approaches reveal complicated pathways. Am J Hum Genet 94:161–175.

Gavrin LK, Denny RA, Saiah E. 2012. Small molecules that target protein misfolding. J Med Chem 55:10823–10843.
Grunewald S. 2009. The clinical spectrum of phosphomannomutase 2 deficiency (CDG-Ia). Biochim Biophys Acta 1792:827–834.
Grunewald S, Schollen E, Van Schaftingen E, Jaeken J, Matthijs G. 2001. High residual activity of PMM2 in patients' fibroblasts: possible pitfall in the diagnosis of CDG-Ia (phosphomannomutase deficiency). Am J Hum Genet 68:347–354.
Hann M, Hudson B, Lewell X, Lifely R, Miller L, Ramsden N. 1999. Strategic pooling of compounds for high-throughput screening. J Chem Inf Comput Sci 39:897–902.
Huth JR, Mendoza R, Olejniczak ET, Johnson RW, Cothron DA, Liu Y, Lerner CG, Chen J, Hajduk PJ. 2005. ALARM NMR: a rapid and robust experimental method to detect reactive false positives in biochemical screens. J Am Chem Soc 127:217–224.
Jaeken J. 2010. Congenital disorders of glycosylation. Ann NY Acad Sci 1214:190–198.
Jorge-Finnigan A, Brasil S, Underhaug J, Ruiz-Sala P, Merinero B, Banerjee R, Desviat LR, Ugarte M, Martinez A, Perez B. 2013. Pharmacological chaperones as a potential therapeutic option in methylmalonic aciduria cblB type. Hum Mol Genet 22:3680–3689.
Levy HL, Milanowski A, Chakrapani A, Cleary M, Lee P, Trefz FK, Whitley CB, Feillet F, Feigenbaum AS, Bebchuk JD et al. 2007. Efficacy of sapropterin dihydrochloride (tetrahydrobiopterin, 6R-BH4) for reduction of phenylalanine concentration in patients with phenylketonuria: a phase III randomised placebo-controlled study. Lancet 370:504–510.
Matthijs G, Schollen E, Bjursell C, Erlandson A, Freeze H, Imtiaz F, Kjaergaard S, Martinsson T, Schwartz M, Seta N et al. 2000. Mutations in PMM2 that cause congenital disorders of glycosylation, type Ia (CDG-Ia). Hum Mutat 16:386–394.
Mu TW, Ong DS, Wang YJ, Balch WE, Yates JR, 3rd, Segatori L, Kelly JW. 2008. Chemical and biological approaches synergize to ameliorate protein-folding diseases. Cell 134:769–781.
Muntau AC, Leandro J, Staudigl M, Mayer F, Gersting SW. 2014. Innovative strategies to treat protein misfolding in inborn errors of metabolism: pharmacological chaperones and proteostasis regulators. J Inherit Metab Dis 37:505–523.
Niesen FH, Berglund H, Vedadi M. 2007. The use of differential scanning fluorimetry to detect ligand interactions that promote protein stability. Nat Protoc 2:2212–2221.
Oprea TI, Zamora I, Ungell AL. 2002. Pharmacokinetically based mapping device for chemical space navigation. J Comb Chem 4:258–266.
Panicker LM, Miller D, Awad O, Bose V, Lun Y, Park TS, Zambidis ET, Sgambato JA, Feldman RA. 2014. Gaucher iPSC-derived macrophages produce elevated levels of inflammatory mediators and serve as a new platform for therapeutic development. Stem Cells 32:2338–2349.
Perez B, Briones P, Quelhas D, Artuch R, Vega AI, Quintana E, Gort L, Ecay MJ, Matthijs G, Ugarte M et al. 2011. The molecular landscape of phosphomannose mutase deficiency in iberian peninsula: identification of 15 population-specific mutations. JIMD Rep 1:117–123.
Pey AL, Desviat LR, Gamez A, Ugarte M, Perez B. 2003. Phenylketonuria: genotype-phenotype correlations based on expression analysis of structural and functional mutations in PAH. Hum Mutat 21:370–378.
Pey AL, Ying M, Cremades N, Velazquez-Campoy A, Scherer T, Thony B, Sancho J, Martinez A. 2008. Identification of pharmacological chaperones as potential therapeutic agents to treat phenylketonuria. J Clin Invest 118:2858–2867.
Powers ET, Morimoto RI, Dillin A, Kelly JW, Balch WE. 2009. Biological and chemical approaches to diseases of proteostasis deficiency. Annu Rev Biochem 78:959–991.
Schneider A, Thiel C, Rindermann J, DeRossi C, Popovici D, Hoffmann GF, Grone HJ, Korner C. 2012. Successful prenatal mannose treatment for congenital disorder of glycosylation-Ia in mice. Nat Med 18:71–73.
Schollen E, Kjaergaard S, Legius E, Schwartz M, Matthijs G. 2000. Lack of Hardy-Weinberg equilibrium for the most prevalent PMM2 mutation in CDG-Ia (congenital disorders of glycosylation type Ia). Eur J Hum Genet 8:367–371.
Serrano M, de Diego V, Muchart J, Cuadras D, Felipe A, Macaya A, Velazquez R, Poo MP, Fons C, O'Callaghan MM et al. 2015. Phosphomannomutase deficiency (PMM2-CDG): ataxia and cerebellar assessment. Orphanet J Rare Dis 10: 138.
Sharma V, Ichikawa M, He P, Scott DA, Bravo Y, Dahl R, Ng BG, Cosford ND, Freeze HH. 2011. Phosphomannose isomerase inhibitors improve N-glycosylation in selected phosphomannomutase-deficient fibroblasts. J Biol Chem 286:39431–39438.
Stenson PD, Mort M, Ball EV, Shaw K, Phillips A, Cooper DN. 2014. The Human Gene Mutation Database: building a comprehensive mutation repository for clinical and molecular genetics, diagnostic testing and personalized genomic medicine. Hum Genet 133:1–9.
Stevens RC, Sancho J, Martinez A. 2010. Rescue of misfolded proteins and stabilization by small molecules. Methods Mol Biol 648:313–324.
Studier FW. 2005. Protein production by auto-induction in high density shaking cultures. Protein Expr Purif 41:207–234.
Summerfield SG, Read K, Begley DJ, Obradovic T, Hidalgo IJ, Coggon S, Lewis AV, Porter RA, Jeffrey P. 2007. Central nervous system drug disposition: the relationship between in situ brain permeability and brain free fraction. J Pharmacol Exp Ther 322:205–213.
Thiel C, Lubke T, Matthijs G, von Figura K, Korner C. 2006. Targeted disruption of the mouse phosphomannomutase 2 gene causes early embryonic lethality. Mol Cell Biol 26:5615–5620.
Tiscornia G, Vivas EL, Matalonga L, Berniakovich I, Barragan Monasterio M, Eguizabal C, Gort L, Gonzalez F, Ortiz Mellet C, Garcia Fernandez JM et al. 2013. Neuronopathic Gaucher's disease: induced pluripotent stem cells for disease modelling and testing chaperone activity of small compounds. Hum Mol Genet 22:633–645.
Tomasic T, Peterlin Masic L. 2012. Rhodanine as a scaffold in drug discovery: a critical review of its biological activities and mechanisms of target modulation. Expert Opin Drug Discov 7:549–560.
Van Schaftingen E, Jaeken J. 1995. Phosphomannomutase deficiency is a cause of carbohydrate-deficient glycoprotein syndrome type I. FEBS Lett 377:318–320.
Vega AI, Perez-Cerda C, Desviat LR, Matthijs G, Ugarte M, Perez B. 2009. Functional analysis of three splicing mutations identified in the PMM2 gene: toward a new therapy for congenital disorder of glycosylation type Ia. Hum Mutat 30:795–803.
Yuste-Checa P, Gamez A, Brasil S, Desviat LR, Ugarte M, Perez-Cerda C, Perez B. 2015. The effects of PMM2-CDG-causing mutations on the folding, activity, and stability of the PMM2 protein. Hum Mutat 36:851:860.